Applied Catalysis B: Environmental 162 (2015) 158–166

Contents lists available at ScienceDirect

Applied Catalysis B: Environmental

journal homepage: www.elsevier.com/locate/apcatb

Kinetics of ammonia consumption during the selective catalytic reduction of NO_x over an iron zeolite catalyst

V. Bacher[a], C. Perbandt[b], M. Schwefer[b], R. Siefert[b], S. Pinnow[b], T. Turek[a,*]

[a] Institute of Chemical Process Engineering, Clausthal University of Technology, 38678 Clausthal-Zellerfeld, Germany
[b] ThyssenKrupp Industrial Solutions AG, 44141 Dortmund, Germany

ARTICLE INFO

Article history:
Received 20 February 2014
Received in revised form 18 June 2014
Accepted 23 June 2014
Available online 30 June 2014

Keywords:
Nitrogen oxides
Selective catalytic reduction
Ammonia oxidation
Iron zeolite
Kinetics

ABSTRACT

The steady-state kinetics of the selective catalytic reduction (SCR) of nitrogen oxides (NO and NO_2) with ammonia over a commercial iron zeolite catalyst were studied in the temperature range of 250 to 450 °C using an integral tubular reactor. Special attention was paid to the stoichiometric ratio of the conversion of ammonia and nitrogen oxides. For this purpose, both systematic SCR measurements at different feed gas compositions and independent studies of the catalytic oxidation of ammonia in the absence of NO and NO_2 were carried out. Under all reaction conditions, a considerable deviation from the expected 1:1 stoichiometry was observed. The steady-state kinetics of the reacting system could be described by global Langmuir–Hinshelwood-type rate equations for *standard* SCR, *fast* SCR, NO/NO_2 equilibrium and NH_3 oxidation. For the correct calculation of the ammonia oxidation it was necessary to include two terms. A first one describing the reaction of NH_3 with O_2, which becomes important at temperatures above 400 °C, and a second rate equation which is not only proportional to NH_3 and O_2 but also to the NO concentration and which is of particular relevance at low reaction temperatures. Additional measurements with different catalyst particle sizes including industrial extrudates could be successfully described with the aid of a reactor model which took film and pore diffusion phenomena into account.

1. Introduction

Iron exchanged zeolites are highly efficient catalysts for the reduction of NO_x (NO and NO_2) with ammonia. As non-toxic materials with similarly high nitrogen oxides reduction activity as the classical vanadia–titania catalyst, iron zeolites are now being widely used for the removal of NO_x from automotive exhaust streams [1]. In addition to NO_x removal, iron zeolites are also capable of decomposing or reducing N_2O very efficiently. Based on these unique properties, the EnviNOx® process for the combined catalytic destruction of all types of nitrogen oxide present in nitric acid tail gases has been developed [2]. Proper design of processes for automotive and stationary removal of nitrogen oxides necessitates the development of kinetic models for the exact calculation of the nitrogen oxide removal rates and the corresponding required amount of the reducing agent ammonia. It is generally accepted that several stoichiometric equations must be considered for successful description of the kinetics of the selective catalytic reaction (SCR) of nitrogen oxides. Nitric oxide reacts with oxygen and ammonia according to the so-called *standard* SCR reaction:

$$4NO + 4NH_3 + O_2 \rightarrow 4N_2 + 6H_2O \quad (R1)$$

while in the presence of nitrogen dioxide the *fast* SCR (R2) with a much higher reaction rate prevails.

$$2NO + 2NO_2 + 4NH_3 \rightarrow 4N_2 + 6H_2O \quad (R2)$$

Even in the absence of NO_2 in the exhaust gas, the *fast* SCR must be taken into account since iron zeolites exhibit a certain catalytic activity for the equilibrium reaction between NO and NO_2:

$$NO + ½O_2 \rightleftarrows NO_2 \quad (R3)$$

If the NO_2:NO_x ratio is below about 50%, the direct reaction of NO_2 with ammonia can be neglected due to the *fast* SCR proceeding much more rapidly [3]. Furthermore, the reducing agent ammonia undergoes catalytic oxidation towards N_2 in the presence of O_2, especially at higher reaction temperatures:

$$4NH_3 + 3O_2 \rightarrow 2N_2 + 6H_2O \quad (R4)$$

* Corresponding author. Tel.: +49 5323 722184; fax: +49 5323 722182.
E-mail addresses: bacher@icvt.tu-clausthal.de (V. Bacher), christian.perbandt@thyssenkrupp.com (C. Perbandt), meinhard.schwefer@thyssenkrupp.com (M. Schwefer), rolf.siefert@thyssenkrupp.com (R. Siefert), stefan.pinnow@thyssenkrupp.com (S. Pinnow), turek@icvt.tu-clausthal.de (T. Turek).

http://dx.doi.org/10.1016/j.apcatb.2014.06.039
0926-3373/

Nomenclature

a	volume specific geometric catalyst surface area (m^{-1})
$c_{G,i}$	gas-phase concentration of species i (mol/m^3)
$c_{S,i}$	catalyst concentration of species i (mol/m^3)
$D_{e,i}$	effective diffusivity of species i (m^2/s)
$E_{A,j}$	activation energy of reaction j (J/mol)
$k_{0,j}$	frequency factor of reaction j (different)
K_i	adsorption constant for species i (different)
n_i	reaction order for species i (–)
r_j	rate of reaction j (mol/(kg s))
R_{sph}	equivalent radius of catalyst particle (m)
R	ideal gas constant (8.3145 J/(mol K))
T	temperature (K)
$u_{G,0}$	superficial gas velocity (m/s)
x	internal catalyst coordinate (m)
z	axial reactor coordinate (m)
β_i	mass transfer coefficient of species i (m/s)
$\nu_{i,j}$	stoichiometric coefficient of species i in reaction j (–)
ρ_{cat}	apparent catalyst density (kg/m^3)

Several models have been developed to describe the kinetics of the catalytic reduction of nitrogen oxides over iron exchanged zeolites, both for steady-state and transient conditions. Extensive work by Tronconi and coworkers has shown that many features of the SCR kinetics on vanadia–titania catalysts can be transferred to iron zeolite catalysts [4–8]. It is generally accepted that ammonia adsorbs strongly under reaction conditions while different adsorbed nitrogen oxides species are discussed as reaction intermediates [3].

One of the remaining unresolved questions regarding the kinetics of SCR on iron zeolites is related to the stoichiometry of the reaction between ammonia and nitrogen oxides. Sachtler and coworkers [9] have raised the question of the SCR stoichiometry. These authors pointed out that the direct reaction of NO with NH_3 would result in an NH_3:NO ratio of 0.66 according to

$$6NO + 4NH_3 \rightarrow 5N_2 + 6H_2O \quad (R5)$$

if NO is not oxidized to NO_2 and NH_3 does not react with O_2. On the other hand, if NO is rapidly oxidized and NO_2 the sole oxidant, the following reaction with a stoichiometric ratio of 1.33 would be obtained:

$$6NO_2 + 8NH_3 \rightarrow 7N_2 + 12H_2O \quad (R6)$$

During their experimental investigations, these authors observed that a molar excess of 10 to 40% of NH_3 was required to reduce a certain amount of NO_x [9]. Devadas et al. [10] have also shown that significant deviations from the postulated stoichiometry of 1:1 according to reactions (R1) and (R2) occur. These authors, and later also Wang et al. [11], suggested that the observed excess NH_3 consumption is caused by the ammonia oxidation reaction (R4). However, Schuler et al. [12,13] demonstrated that this cannot be the only reason as the over-consumption of ammonia is more pronounced at lower temperatures where the relatively slow ammonia oxidation does not take place to a significant extent. Schuler et al. postulated that either a surface species might be formed during *standard* SCR which passes through a redox cycle consuming NH_3 for reduction and O_2 for oxidation [12] or that ammonia could be decomposed to the elements [13]. In these studies, the stoichiometric deviations were accounted for modeling purposes by empirical temperature-dependent factors. Markatou et al. [14] presented a kinetic model for SCR over iron zeolite catalysts and incorporated the ammonia oxidation not only to nitrogen (R4) but also to nitric oxide:

$$4NH_3 + 5O_2 \rightarrow 4NO + 6H_2O \quad (R7)$$

Sjövall et al. [15] introduced, in addition to *standard* SCR (R1) and ammonia oxidation (R4), a further stoichiometric equation

$$12NH_3 + 10NO + 4O_2 \rightarrow 11N_2 + 18H_2O \quad (R8)$$

which results in a constant additional ammonia demand of 20% for each mole of NO converted. Colombo et al. incorporated the concentration of NO as additional term in their kinetic expression for reaction (R4) [16]. This approach results in an acceleration of the ammonia oxidation whenever NO is present. Very recently, Olsson and coworkers presented mechanistic evidence – by careful studies with isotopically labeled reactants – that the parasitic oxidation of NH_3 occurring at low temperatures is enhanced in the presence of NO [17]. These authors proposed that reaction (R7) yielding NO is mainly responsible for this effect, although the oxidation of ammonia to nitrogen according to reaction (R4) could not be ruled out.

In our contribution a refined approach for the description of the ammonia oxidation kinetics during the SCR of nitrogen oxides is presented. We introduce a second term in the ammonia oxidation rate equation which is not only dependent on the NH_3 and O_2 concentrations, but also a function of the NO content. This approach reflects an NH_3 consuming redox cycle without reduction of NO as proposed by Schuler et al. [12]. Consequently, the activation energy of the additional reaction is allowed to differ from the value for the ammonia oxidation reaction with O_2 in the absence of NO. Since the aim of the study is the description of steady-state catalyst operation, global Langmuir–Hinshelwood-type rate equations are used. It will be shown that this kinetic approach is capable of describing the NH_3:NO_x stoichiometry with good accuracy over a broad range of temperatures and concentrations of NO, NO_2, NH_3 and O_2. Moreover, the influence of mass transfer resistances during measurements with different catalyst sieve fractions can also be successfully described.

2. Methods

2.1. Experimental

The experiments were carried out with a commercial iron zeolite catalyst (Clariant Produkte (Deutschland) GmbH, EnviCat®-NO_x). Details of the experimental method have been described elsewhere [18]. Briefly, catalyst extrudates that had been kept under working conditions in a nitric acid exhaust gas stream for three months were used as received or crushed and sieved to different fractions. The exact shape of the catalyst bodies is proprietary and cannot be disclosed. If not otherwise noted, the measurements were performed with 0.94 g of these fractions diluted with the same volume of glass beads or silicon carbide particles (315 to 500 μm) and loaded into a tubular stainless steel reactor (18 mm ID) that was coated with silica through a sol–gel method to prevent ammonia oxidation at the reactor wall. In blank tests with an uncoated stainless steel reactor it was found that considerable amounts of NH_3 reacted above temperatures of 350 °C.

Reactant mixtures with a total flow rate of 2000 cm^3/min (NTP) were obtained by feeding NO, NO_2, NH_3, H_2O, O_2 and N_2 via mass flow controllers (Bronkhorst High-Tech) at an absolute reactor pressure of 1.7 bar which was maintained with a regulating valve (Bronkhorst High-Tech). Gas analysis of inlet and outlet reactor streams was carried out with an FTIR spectrometer (Nicolet 5700, Thermo Scientific) and an oxygen analyzer (Oxymat 6, Siemens). The reactions were studied at temperatures from 250 to 450 °C

with feeds containing 0 to 400 ppm NO, 0 to 125 ppm NO_2, 104 to 962 ppm NH_3, 1.2 to 4.0 vol% O_2 and 0.16 to 2.0 vol% H_2O balanced in N_2.

2.2. Kinetic analysis of measured data

The measured reactant concentrations at the reactor outlet were analyzed with a steady-state, heterogeneous 1D + 1D reactor model. Given the low heats of reaction in the diluted gas streams, isothermal reactor operation was assumed. The lengths of the catalytic packings were sufficiently high to ensure plug flow behavior at Bodenstein numbers (or reactor Peclet numbers) larger than 100 [19]. Pressure drop and density changes of the gas flow were neglected. The following mass balance equations and boundary conditions were used:

- Gas phase

$$\text{Mass balance} \quad u_{G,0}\frac{dc_{G,i}}{dz} = -\beta_i a(c_{G,i} - c_{S,i}) \tag{1}$$

$$\text{Boundary condition} \quad (z = 0) \quad c_{G,i} = c_{G,i,0} \tag{2}$$

Here, $u_{G,0}$ is the superficial gas velocity, z the axial reactor coordinate and a the average value of the specific geometric catalyst surface area assuming spherical geometry. $c_{G,i}$ and $c_{S,i}$ are the reactant concentrations in the gas phase and at the outer catalyst surface, respectively. The mass transfer coefficients β_i for packed beds were calculated from Sherwood numbers, which were determined in analogy to Nußelt numbers [20]. The required molecular diffusion coefficients were obtained from Massman [21].

- Catalyst phase

$$\text{Mass balance} \quad D_{e,i}\frac{d^2c_{S,i}}{dx^2} = -\rho_{cat}\sum_j \nu_{i,j} r_j \tag{3}$$

$$\text{Boundary condition} \quad (x = 0) \quad \frac{dc_{S,i}}{dx} = 0 \tag{4}$$

$$\text{Boundary condition} \quad (x = R_{sph}) \quad D_{e,i}\frac{dc_{S,i}}{dx} = \beta_i a(c_{G,i} - c_{S,i}) \tag{5}$$

Here, x is the internal catalyst coordinate, R_{sph} the equivalent radius of the catalyst particles, ρ_{cat} the apparent catalyst density, $D_{e,i}$ the effective diffusivity and $\nu_{i,j}$ the stoichiometric coefficient of species i in reaction j. Note that Eq. (3) is derived for slab geometry of the catalyst. Thus, the equivalent catalyst radius is an approximate measure for the characteristic diffusion length. For the calculation of the effective diffusivities both pore and Knudsen diffusion were taken into account. The kinetic parameters in the expressions for the reaction rates r_j were determined by the fitting of measured outlet reactor concentrations with the software package Presto-Kinetics. The temperature dependence of the rate constants was described by the Arrhenius equation.

$$k_j = k_{0,j}\exp\left(\frac{-E_{A,j}}{RT}\right) \tag{6}$$

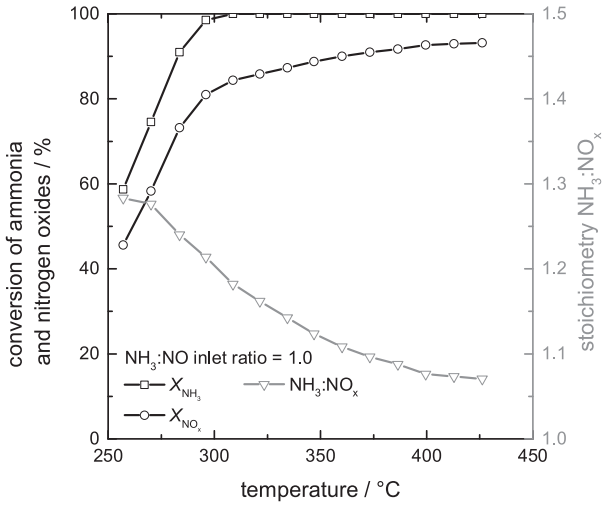

Fig. 1. NH_3 and NO conversions as well as stoichiometric ratio of converted NH_3 and NO_x amounts as a function of temperature for an equimolar reactant mixture. 2.5 vol% O_2, 400 ppm NO, 400 ppm NH_3 and 3100 ppm H_2O at reactor inlet, catalyst sieve fraction 315–500 μm.

3. Results and discussion

3.1. Observed stoichiometry of the reaction of NH_3 with nitrogen oxides

Fig. 1 shows an example of the observed NH_3 and NO conversions for an equimolar reactant mixture as a function of temperature. In agreement with earlier studies it can be clearly seen that strong deviations from the 1:1 stoichiometry according

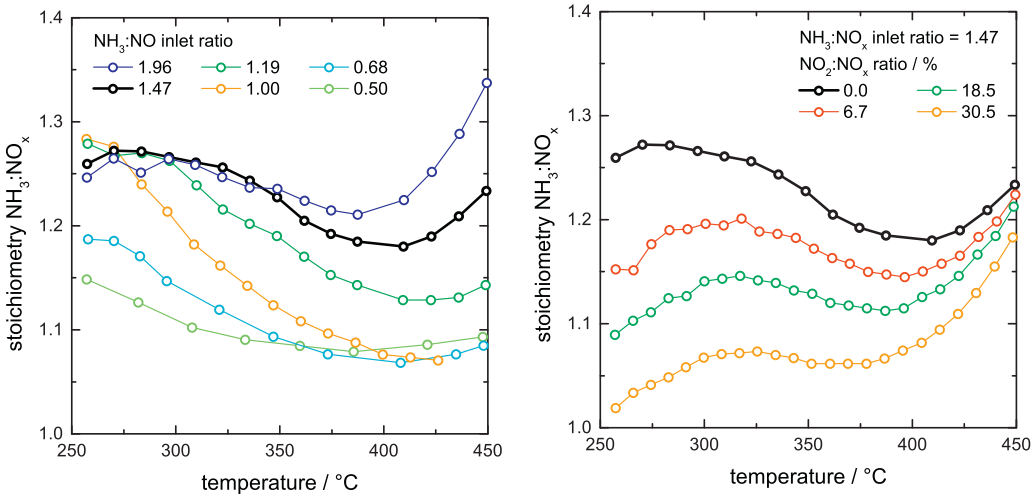

Fig. 2. Stoichiometric ratio of converted NH_3 and NO_x amounts as a function of temperature at different ammonia to nitrogen oxides ratios without NO_2 at reactor inlet (left) and for different NO_2:NO_x ratios at an NH_3:NO_x ratio of 1.47 (right). 2.5 vol% O_2, 400 ppm NO_x and 3100 ppm H_2O at reactor inlet, catalyst sieve fraction 315–500 μm.

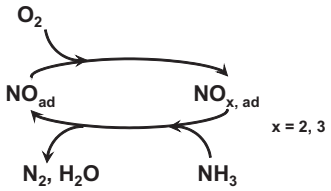

Fig. 3. Proposed catalytic redox cycle for the NO assisted NH_3 oxidation based on the work of Schuler [12,13].

to the reactions (R1) and (R2) occur over the whole temperature range. However, the stoichiometric ratio between the converted amounts of ammonia and NO is also dependent on temperature with significant deviations of up to 30% especially at low temperatures. Further results of the stoichiometric ratio between the converted amounts of ammonia and NO_x during SCR measurements are presented in Fig. 2 as a function of temperature. The required stoichiometric ammonia excess ranges from less than 5% to more than 35% depending on the reaction conditions employed.

The left hand side of Fig. 2 shows that the relative ammonia consumption is enhanced by the stoichiometric feed ratio of the reactants. This positive effect of ammonia concentration on the reductant overconsumption is in agreement with Nedyalkova et al. [17]. The ratio of the converted NH_3:NO_x amounts decreases with rising temperature below about 400 °C. This effect cannot be explained by the catalytic oxidation of NH_3 with O_2, as this reaction becomes more and more effective with increasing temperature and is therefore only responsible for the increase of the stoichiometric ratio at higher temperatures, i.e. >400 °C, as will be shown later.

The variation of the NO_2:NO_x ratio at the reactor inlet also reveals interesting trends (Fig. 2, right). Here it can be seen that the addition of NO_2 strongly improves the ammonia selectivity at temperatures lower than required for ammonia oxidation with O_2 (above 400 °C). Thus, the deviation of the expected 1:1 stoichiometry at low temperatures is evidently enhanced by the presence of high NO concentrations. These findings, which are in agreement with Colombo et al. [16] and Nedyalkova et al. [17], could be explained by a catalytic redox cycle involving NO and adsorbed NO_x species (Fig. 3) during which NH_3 is oxidized by O_2 [12,13].

3.2. Kinetic simulation of NO_x reduction including NH_3 oxidation in the absence and presence of NO

In order to kinetically simulate the overall reaction network those reactions which could be measured independently were investigated first. These were the equilibrium reaction between NO and NO_2 (R3), the kinetics of which had been described in a previous paper [18], and the catalytic oxidation of NH_3 in the absence of nitrogen oxides which is described in the following section.

3.2.1. Kinetics of the catalytic oxidation of NH_3

The oxidation of ammonia in the absence of nitrogen oxides was studied in a series of independent measurements over a range of temperatures and reactant concentrations. Due to the relatively low reaction rates, the amount of catalyst had to be increased to 5.97 g which was used without dilution in the reactor. The results can be described with very good accuracy using the kinetic expression given in Table 1 as can be seen from the comparison between calculated and measured results obtained at different water vapor concentrations (Fig. 4, left) and ammonia feed compositions (Fig. 4, right).

Table 1
Concentration dependency in rate equations and kinetic parameters.

Concentration dependency $f(c_i)$ in rate equation	k_0	E_A/kJ/mol	Reaction orders	Adsorption constants
Standard SCR (R1) $\left(c_{NO}{}^{n_{NH_3}} c_{O_2}{}^{n_{O_2}}\right) / \left(1 + K_{NH_3} c_{NH_3}^2\right)$	9.13×10^{10} m$^{9.18}$/kg$_{cat}$ s mol$^{2.06}$	66.7	$n_{NH_3} = 1.5$ $n_{O_2} = 0.56$	$K_{NH_3} = 4.73 \times 10^7$ m^6/mol^2
Fast SCR (R2) $c_{NO_2} c_{NO} c_{NH_3}$	5×10^7 m^9/kg$_{cat}$ s mol^2	36		
NO oxidation [18] (R3) $\left(c_{NO}{}^{n_{O_2}} c_{O_2}{}^{n_{O_2}} - \left(c_{NO_2}{}^{n_{O_2}} c_{O_2}{}^{-0.5}\right) / \sqrt{K_c}\right) / \left(1 + K_{NO_2} c_{NO_2} + K_{H_2O} c_{H_2O}{}^{n_{H_2O}}\right)^2$	10.35 m$^{5.25}$/kg$_{cat}$ s mol$^{0.75}$	31	$n_{O_2} = 0.75$ $n_{H_2O} = 0.5$	$K_{NO_2} = 27.9$ m^3/mol $K_{H_2O} = 1.98$ m$^{1.5}$/mol$^{0.5}$ $K_c = c_{NO_2}^2 / \left(c_{NO}^2 c_{O_2}\right)$
NH_3 oxidation with O_2 (R4) $\left(c_{NH_3}{}^{n_{NH_3}} c_{O_2}{}^{n_{O_2}}\right) / \left(1 + K_{H_2O} c_{H_2O}{}^{n_{H_2O}}\right)$	6.83×10^5 mol$^{0.1}$ m$^{2.7}$/kg$_{cat}$ s	96.3	$n_{NH_3} = 0.6$ $n_{O_2} = 0.3$ $n_{H_2O} = 0.3$	$K_{H_2O} = 19.1$ m$^{0.9}$/mol$^{0.3}$
NO assisted NH_3 oxidation (R4) $\left(c_{NO}{}^{n_{NO}} c_{O_2}{}^{n_{O_2}} c_{NH_3}\right) / \left(1 + K_{NH_3} c_{NH_3}^2\right)$	2.58×10^4 m$^{9.03}$/kg$_{cat}$ s mol$^{2.01}$	48	$n_{O_2} = 0.98$ $n_{NO} = 1.03$	$K_{NH_3} = 1.11 \times 10^4$ m^6/mol^2

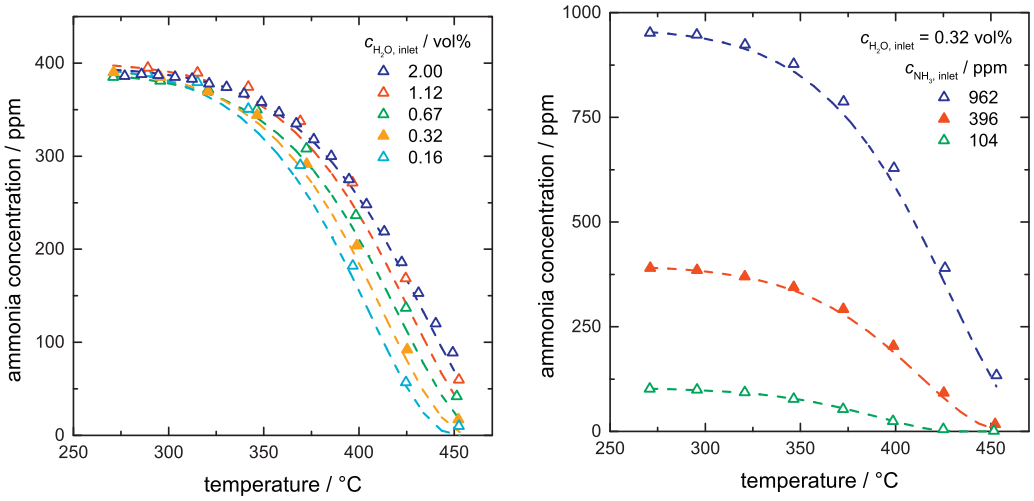

Fig. 4. Measured and calculated NH_3 outlet concentrations as a function of temperature for different water (left) and ammonia (right) concentrations at reactor inlet. 2.5 vol% O_2, 0 ppm NO_x at reactor inlet, catalyst mass 5.97 g, catalyst sieve fraction 315–500 μm. Symbols: measurements, broken lines: simulations.

3.2.2. *Kinetics of the NO assisted selective catalytic oxidation of NH_3*

For analysis of the measured data regarding the ammonia oxidation in the presence of nitrogen oxides, all reactions (R1) to (R4) had to be considered simultaneously. For this purpose the kinetics for NO and NH_3 oxidation were complemented by kinetic descriptions of the NO_x reduction. For the *standard* SCR, a Langmuir–Hinshelwood-type rate equation was used (Table 1). In agreement with the literature [1,4,11–15], the *fast* SCR was assumed to be first order with respect to the concentrations of NO, NO_2 and NH_3. The activation energy for the *fast* SCR was used from Schuler [13] and the frequency factor was determined during the overall parameter fitting. For the NO assisted oxidation of NH_3 it was assumed that this reaction has the same stoichiometry as reaction (R4) and that its reaction rate is proportional to the NO concentration. The underlying physical basis can be derived from the above postulated catalytic redox cycle (Fig. 3), that leads to a concurrent enhancement of ammonia oxidation by O_2. Hence it is assumed that the surface concentration of the adsorbed NO species is proportional to the NO gas phase concentration. All rate equations and the kinetic parameters obtained in the concluding parameter fitting for the overall reaction network are summarized in Table 1.

Fig. 5 shows the comparison between measured and calculated reactor outlet concentrations of NO (left) and NH_3 (right) as a function of temperature for a series of measurements where NO_x was fed as NO only. It can be seen that the measured data are correctly described in a range of NH_3:NO feed ratios between 0.5 and about 2. The left hand side of Fig. 5 reveals that the achievable NO conversion remains significantly below 100% even at high temperatures for NH_3:NO feed ratios $\leq$1. For stoichiometric feed (NH_3:NO = 1, orange symbols), the NO outlet concentration approaches some 30 ppm for high temperatures while NH_3 is already completely consumed at around 300 °C. This shows again to which extent ammonia is excessively consumed during SCR on the iron zeolite catalyst. For NH_3:NO feed ratios exceeding unity, NO conversion always approaches 100%. The required temperature for full NO conversion increases with rising ammonia concentration which can be explained by the inhibiting effect of NH_3 on the rate of the *standard* SCR reaction. An interesting phenomenon can be seen in the right hand diagram of Fig. 5 for an NH_3:NO feed ratio of 1.19. With rising temperature, ammonia reaches almost complete conversion at around 330 °C, but at even higher temperatures, the NH_3 outlet concentration increases again. This phenomenon is caused by the different distribution of NO concentrations in the integral reactor during these measurements and will be interpreted later.

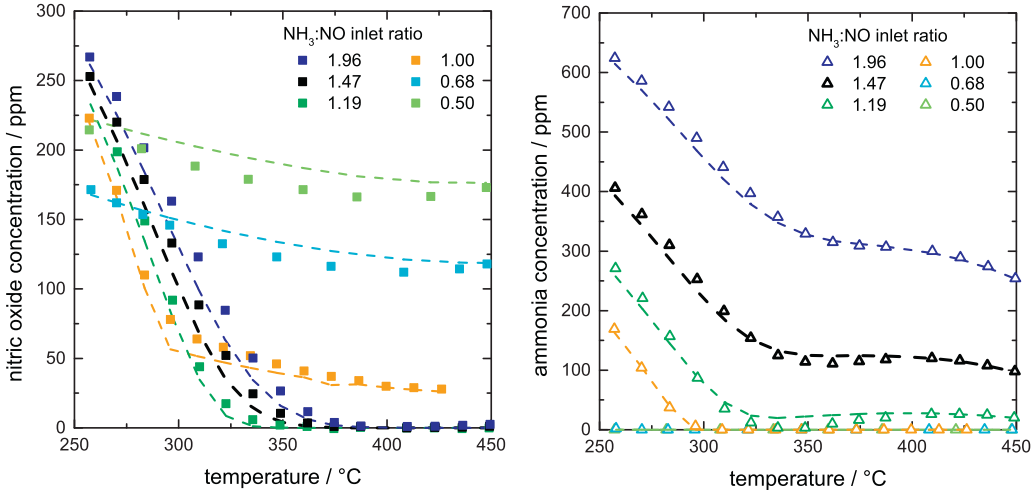

Fig. 5. Measured and calculated outlet concentrations of NO (left) and NH_3 (right) as a function of temperature for different ammonia to nitric oxide ratios at reactor inlet. 2.5 vol% O_2, 400 ppm NO and 3100 ppm H_2O at reactor inlet, catalyst sieve fraction 315–500 μm. Symbols: measurements, broken lines: simulations.

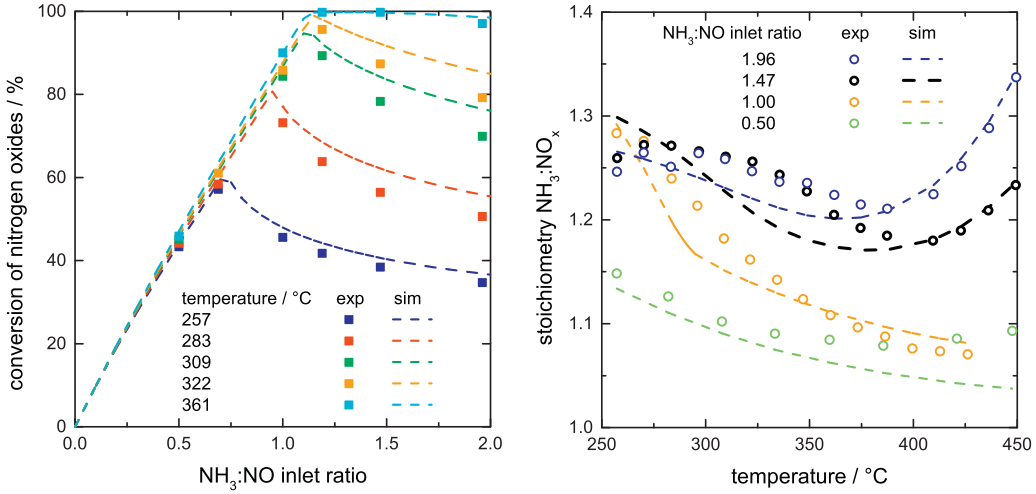

Fig. 6. Measured and calculated NO_x conversions (left) and stoichiometric ratios (right) as a function of the NH_3:NO ratio at reactor inlet at different temperatures. 2.5 vol% O_2, 400 ppm NO, and 3100 ppm H_2O at reactor inlet. Symbols: measurements, broken lines: simulations.

Fig. 6 depicts selected data of the series of measurements shown in Fig. 5 in a different form. In the left hand diagram, the achieved NO_x conversion is plotted as a function of the NH_3:NO ratio at reactor inlet. Here, the deviation from the 1:1 stoichiometry can be recognized by a decreased slope of the curves before reaching the maximum NO_x conversion. The right hand diagram of Fig. 6 reveals a relatively good agreement between measured and calculated stoichiometric ratios of the converted NH_3 and NO amounts.

Comparison of the activation energies determined for the different reactions occurring allows the temperature dependency of the stoichiometric deviations during NH_3 conversion to be explained. Since the NO assisted ammonia oxidation has a low activation energy of 48 kJ/mol, the relative contribution of this reaction path is quite high at low reaction temperatures. With rising temperature, the rate of the *standard* SCR with an activation energy of approx. 67 kJ/mol is accelerated more strongly than the NO assisted NH_3 oxidation, and the stoichiometric ammonia excess decreases. At even higher temperatures, however, the ammonia oxidation by O_2 with the highest activation energy of around 96 kJ/mol gives again rise to larger deviations from the 1:1 stoichiometry.

Results depicted in Fig. 7 reveal that the variation of the oxygen feed concentration can also be successfully modeled with the kinetic equations developed. One can see from the right hand diagram of Fig. 7 that the required ammonia excess increases in the presence of higher O_2 concentrations. While the temperature trend and the minima of the ammonia excess at a temperature of around 400 °C are correctly captured by the kinetic model, the description of the stoichiometric ratio (Fig. 7, right) succeeded in a merely qualitative manner. Regarding the absolute exactness it has to be taken into account that the chosen representation of the data is extremely sensitive to small differences between measured and calculated results.

Further measurements with different mixtures of NO and NO_2 at the reactor inlet were also carried out. The results in Fig. 8 for an NH_3:NO_x ratio of 1.47 at the reactor inlet show that the addition of NO_2 at a constant total NO_x concentration (400 ppm) accelerates the conversion of NH_3 only at temperatures below about 320 °C. This can be easily explained by the enhancing effect of NO_2 through the *fast* SCR. In all cases, no NO_2 could be detected at reactor outlet. However, the remaining ammonia concentration at 350 to 400 °C, where the nitrogen oxides are always completely consumed, is significantly higher for gas mixtures containing NO_2 than in the case of pure NO in the feed. This is due to the enhancing effect of NO on the oxidation of ammonia whereas in the presence of NO_2, NO apparently reacts very fast and thus selectively with NH_3 and NO_2 according to reaction (R2) and leads to an improvement of the required stoichiometric excess of the reducing agent (Fig. 8, right). However, it cannot be derived from our measurements if the

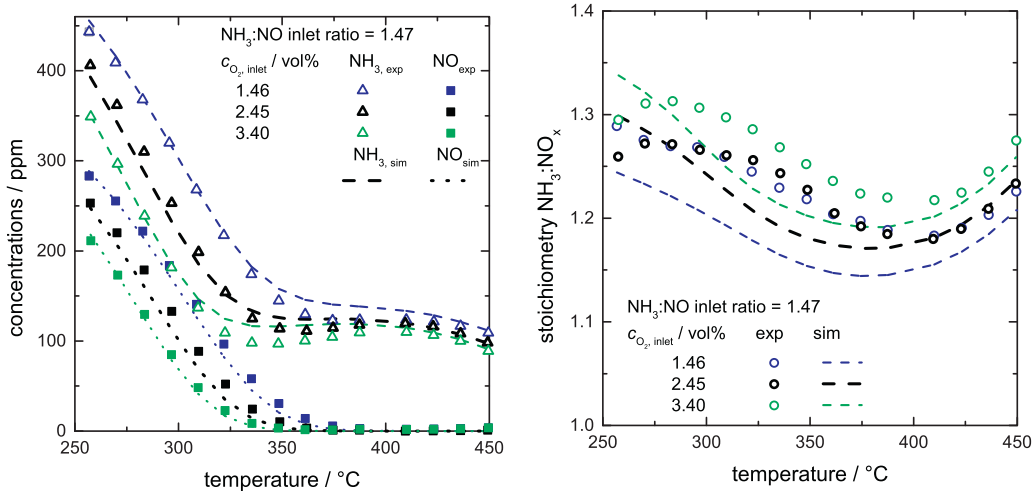

Fig. 7. Measured and calculated outlet concentrations of NO and NH_3 (left) and stoichiometric ratio (right) as a function of temperature for different oxygen concentrations at reactor inlet. 590 ppm NH_3, 400 ppm NO and 3100 ppm H_2O at reactor inlet, catalyst sieve fraction 315–500 μm. Symbols: measurements, broken lines: simulations.

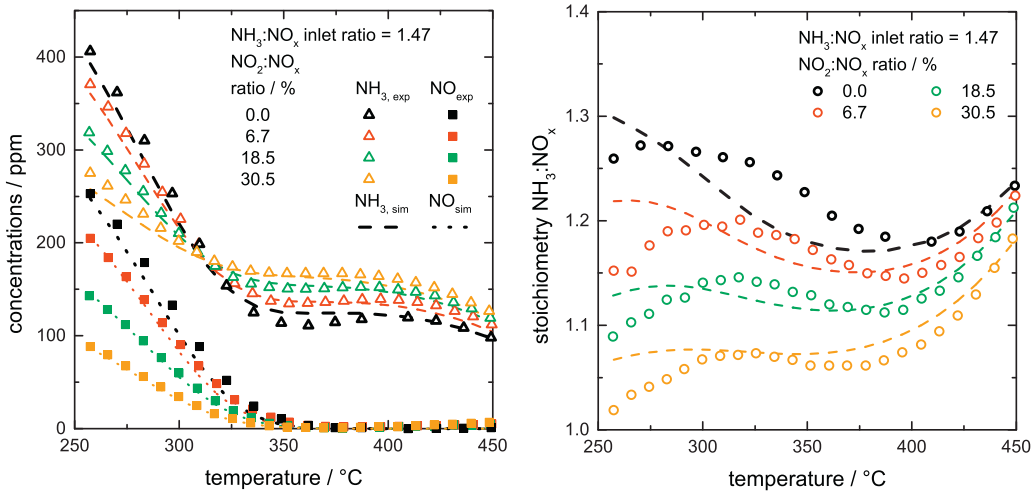

Fig. 8. Measured and calculated outlet concentrations of NO and NH_3 as a function of temperature for different NO_2:NO_x ratios at reactor inlet. 2.5 vol% O_2, 590 ppm NH_3, 400 ppm NO_x and 3100 ppm H_2O at reactor inlet, catalyst sieve fraction 315–500 μm. Symbols: measurements, broken lines: simulations.

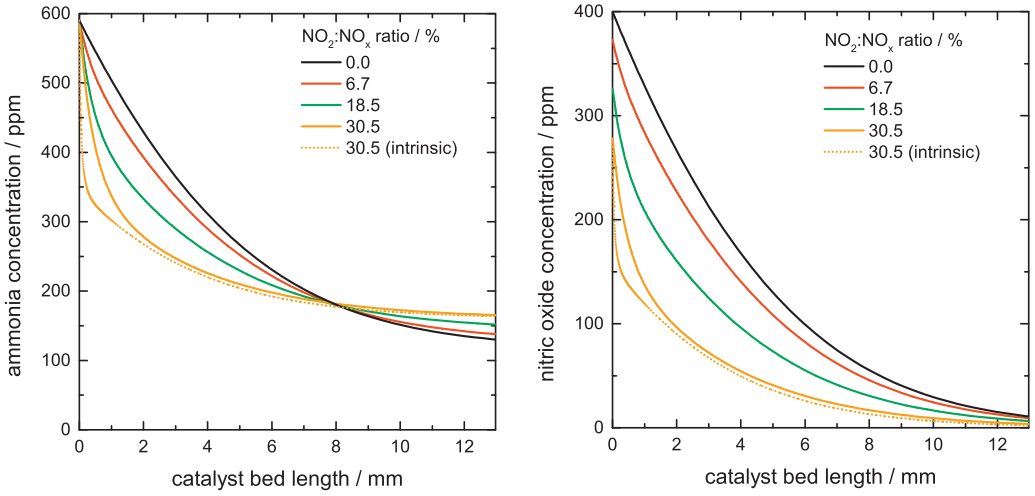

Fig. 9. Calculated concentrations of NH_3 (left) and NO (right) as a function of catalyst bed length for different NO_2:NO_x ratios at reactor inlet. Particle diameter 400 μm, reactor temperature 343 °C, 2.5 vol% O_2, 400 ppm NO_x, 590 ppm NH_3 and 3200 ppm H_2O at reactor inlet.

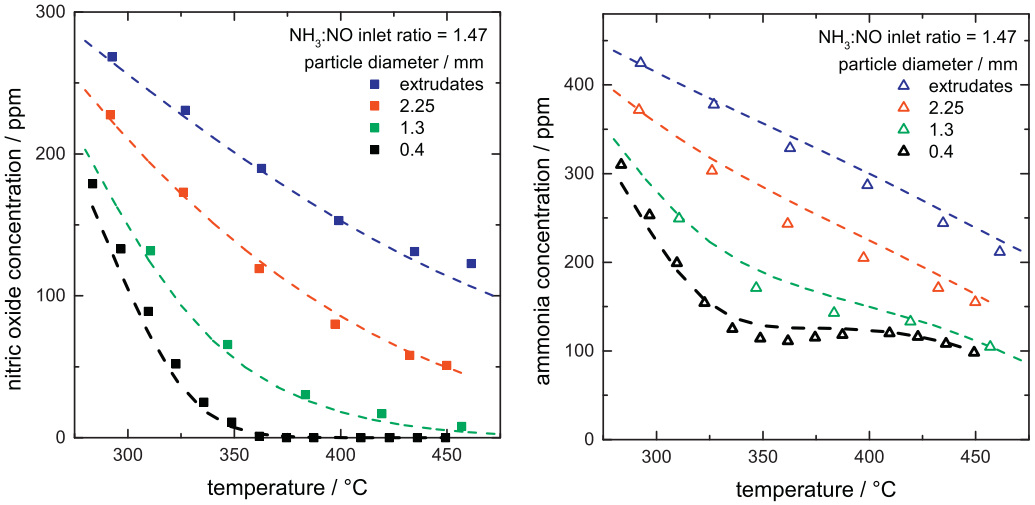

Fig. 10. Measured and calculated outlet concentrations of NO (left) and NH_3 (right) as a function of temperature for different catalyst particle sizes. 2.5 vol% O_2, 400 ppm NO, 590 ppm NH_3 and 3100 ppm H_2O at reactor inlet. Symbols: measurements, broken lines: simulations.

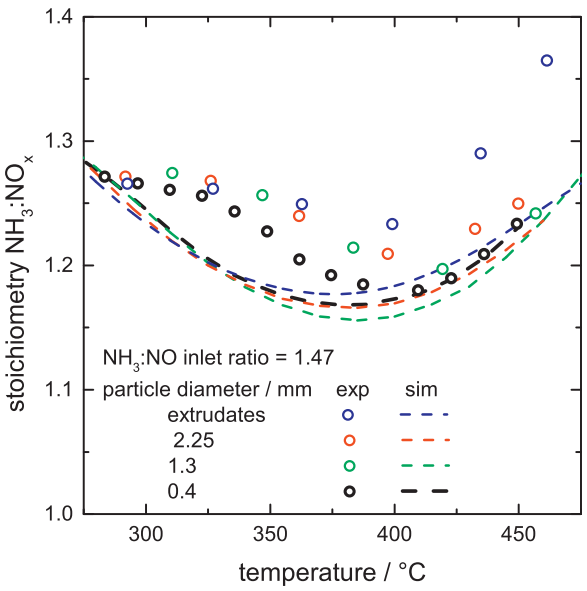

Fig. 11. Measured and calculated stoichiometric NH_3:NO_x ratios as a function of temperature for different catalyst particle sizes. 2.5 vol% O_2, 400 ppm NO, 590 ppm NH_3 and 3100 ppm H_2O at reactor inlet. Symbols: measurements, broken lines: simulations.

NH_3 oxidation is enhanced in the presence of NO_2 since only gas mixtures with NO_2:NO_x ratios lower than 50% were used. In order to achieve a better understanding of the observations, the simulated NH_3 and NO concentrations as a function of reactor length are depicted in Fig. 9 for different NO_2:NO_x ratios at a reactor temperature of 343 °C and feed concentrations of 400 ppm NO_x and 590 ppm NH_3, respectively. The predicted ammonia concentration in the inlet zone of the reactor strongly decreases upon addition of NO_2. However, the ammonia concentration curves intersect each other at a catalyst bed length of about 8 mm while at reactor outlet the sequence of ammonia concentrations is inverted with higher values occurring for NO_2-containing feeds. This can be explained by the corresponding higher average NO concentration levels in the reactor (Fig. 9, right) giving rise to larger amounts of ammonia being oxidized. In a similar manner, the peculiarities of the NH_3 outlet concentration versus temperature during certain measurements depicted in Fig. 5 can be understood. Specifically, the fact that the NH_3 outlet concentration during the measurement with an NH_3:NO inlet ratio of 1.19 (green symbols) reaches almost zero at around 350 °C and then again increases at higher temperatures, is also caused by the corresponding different average NO levels in the reactor.

The diagrams of Fig. 9 also show comparisons between calculated values obtained with the full reactor model and with the intrinsic kinetics in the absence of any mass transfer resistances. Differences can only be seen directly at the reactor inlet, where NO_2 is still present and the extremely rapid *fast* SCR (R2) occurs.

3.3. Influence of catalyst particle diameter

The overall model developed, including mass transport effects, was finally validated with different catalyst sieve fractions including commercial catalyst extrudates. The comparison of measured and calculated NO and NH_3 concentrations at the reactor outlet depicted in Fig. 10 reveals that the influence of film and pore diffusion on the overall reaction rates can be described with good accuracy. The performance of commercial extrudates is drastically diminished compared to the smallest sieve fraction (average diameter 0.4 mm) with which the intrinsic chemical kinetics could be measured over the whole range of conditions studied. While in this case complete NO consumption is always obtained above 350 °C, the extrudates only allow for NO conversions of about 50% (350 °C) to around 75% (450 °C). This shows that small catalyst diffusion lengths (e.g. in coated honeycomb monolith structures) are beneficial for achieving a high utilization of the catalytic material. On the other hand, the simulation reveals that mass transfer resistances have little influence on the required stoichiometric ammonia amount (see Fig. 11). However, the differences resulting from the variation of particle size are considerably smaller than the scatter in the experimental data points.

Overall, the kinetics developed allow the rates of NH_3 and nitrogen oxides conversions to be described with very good accuracy as shown in the parity plots for reactant concentrations (Fig. 12, left) and conversions (Fig. 12, right). The mean deviation between measured and calculated concentrations amounts to 4.5 ppm, which is equivalent to a mean relative error of 8.0% (assuming a detection limit of 5 ppm). Regarding the conversions, we obtained an absolute deviation of only 1.1%. This corresponds to an average relative error of 2.3% (measurements without NO_2 at reactor inlet not taken into account). The used set of data (overall 669) also included the independent measurements for the variation of the catalyst particle diameter.

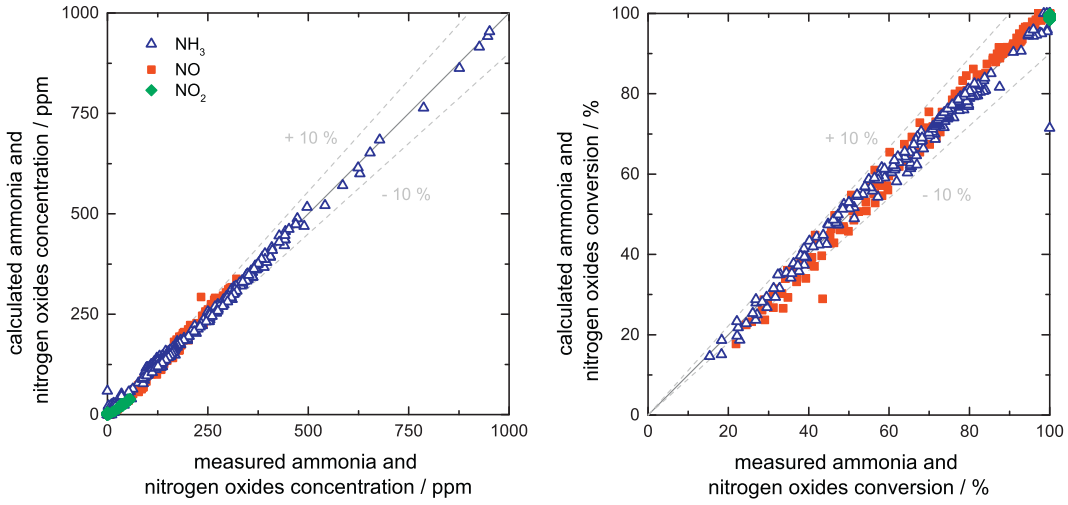

Fig. 12. Parity plot for all measured NH_3 and nitrogen oxides concentrations at reactor outlet (left) as well as for NH_3 and nitrogen oxides conversions (right).

4. Conclusions

Steady-state measurements of the reduction of nitrogen oxides with ammonia in the presence of oxygen were carried out in an integral reactor over a commercial iron zeolite catalyst at different temperatures, concentrations and catalyst particle sizes. The kinetics of the catalytic oxidation of NH_3 with O_2 were determined in separate measurements in the absence of nitrogen oxides. Kinetic analysis of the measured data with global Langmuir–Hinshelwood-type rate equations revealed that the observed deviations from the expected 1:1 stoichiometry of the NH_3–NO reaction cannot be explained only by the parallel reaction of ammonia with oxygen, which is mainly responsible for the increased ammonia oxidation above reaction temperatures of around 400 °C. For successful description of the measurements at lower temperature, a second kinetic expression for the NO assisted ammonia oxidation had to be introduced in which the rate is not only proportional to the NH_3 and O_2 concentrations, but also to the NO concentration. These findings are in agreement with Colombo et al. [16] and Nedyalkova et al. [17] and support earlier suggestions by Schuler et al. [12,13] revealing that NO forms a surface species which passes through a redox cycle and consumes NH_3 for reduction and O_2 for oxidation. It could be furthermore shown that the *fast* SCR is very selective and does not lead to additional ammonia oxidation. Measurements with different catalyst particle sizes revealed that mass transfer resistances strongly affect the overall reaction kinetics, especially for the catalyst extrudates of commercial size. In that case, ammonia oxidation is even more pronounced than under reaction conditions where intrinsic chemical kinetics prevail. The kinetic model developed allows, for the first time, to calculate with good accuracy the amount of ammonia required for the selective catalytic reduction of NO and NO_2 over iron zeolites over a broad range of reaction conditions.

Acknowledgements

The authors would like to thank Clariant Produkte (Deutschland) GmbH for kindly providing the catalyst samples and ThyssenKrupp Industrial Solutions AG for their financial support.

References

[1] D. Chatterjee, P. Kočí, V. Schmeißer, M. Marek, M. Weibel, B. Krutzsch, Catal. Today 151 (2010) 395–409.
[2] M.C.E. Groves, A. Sasonow, J. Integr. Environ. Sci. 7 (2010) 211–222.
[3] S. Brandenberger, O. Kröcher, A. Tissler, R. Althoff, Catal. Rev. Sci. Eng. 50 (2008) 492–531.
[4] D. Chatterjee, T. Burkhardt, M. Weibel, I. Nova, A. Grossale, E. Tronconi, Numerical Simulation of Zeolite- and V-Based SCR-Catalytic Converters, SAE Technical Paper 2007-01-1136, ISBN 0-7680-1635-5.
[5] D. Chatterjee, T. Burkhardt, M. Weibel, E. Tronconi, I. Nova, C. Ciardelli, Numerical Simulation of NO/NO_2/NH_3 Reactions on SCR-Catalytic Converters: Model Development and Applications, SAE Technical Paper 2006-01-0468, ISBN 0-7680-1758-0.
[6] I. Nova, C. Ciardelli, E. Tronconi, D. Chatterjee, M. Weibel, Top. Catal. 42–43 (2007) 43–46.
[7] A. Grossale, I. Nova, E. Tronconi, Catal. Today 136 (2008) 18–27.
[8] A. Grossale, I. Nova, E. Tronconi, D. Chatterjee, M. Weibel, J. Catal. 256 (2008) 312–322.
[9] Q. Sun, Z.-X. Gao, H.-Y. Chen, W.M.H. Sachtler, J. Catal. 201 (2001) 88–99.
[10] M. Devadas, O. Kröcher, A. Wokaun, React. Kinet. Catal. Lett. 86 (2005) 347–354.
[11] T.J. Wang, S.W. Baek, H.J. Kwon, Y.J. Kim, I.-S. Nam, M.-S. Cha, G.K. Yeo, Ind. Eng. Chem. Res. 50 (2011) 2850–2860.
[12] A. Schuler, M. Votsmeier, P. Kiwic, J. Gieshoff, W. Hauptmann, A. Drochner, H. Vogel, Chem. Eng. J. 154 (2009) 333–340.
[13] A. Schuler, Selektive katalytische Reduktion von Stickoxiden mit Ammoniak an Fe-Zeolith-Katalysatoren, Dissertation, TU Darmstadt, Darmstadt, 2009.
[14] P. Markatou, J. Dai, A. Johansson, W. Klink, M. Castagnola, T.C. Watling, M. Tutuianu, SAE Technical Paper 2011-01-1304.
[15] H. Sjövall, R.J. Blint, A. Gopinath, L. Olsson, Ind. Eng. Chem. Res. 49 (2010) 39–52.
[16] M. Colombo, I. Nova, E. Tronconi, V. Schmeißer, B. Bandl-Konrad, L. Zimmermann, Appl. Catal., B: Environ. 111–112 (2012) 106–118.
[17] R. Nedyalkova, K. Kamasamudram, N.W. Currier, J. Li, A. Yezerets, L. Olsson, J. Catal. 299 (2013) 101–108.
[18] V. Bacher, C. Perbandt, M. Schwefer, R. Siefert, T. Turek, Appl. Catal., B: Environ. 134–135 (2013) 55–60.
[19] H.S. Fogler, Elements of Chemical Reaction Engineering, third ed., Prentice Hall, Upper Saddle River, New Jersey, 1999 (Chapter 14.2).
[20] V.D.I. Heat, Atlas, 10th ed., VDI-Verlag, Berlin, 2006 (Chapter Gj2).
[21] W.J. Massman, Atmos. Environ. 32 (1998) 1111–1120.